

Article

Functionalized Coal Fly Ash Is an Efficient Catalyst for Synthesizing Furfural from Xylose at a Low Catalyst Load

Mengling Li, Ye Wang, Lin Liu, Yanan Gao, Zhanyun Gao and Liping Zhang *

Department of Chemistry and Chemical Engineering, MOE Engineering Research Center of Forestry Biomass Materials and Bioenergy, Beijing Forestry University, Beijing 100083, China; limengling@bjfu.edu.cn (M.L.); wangye1220@bjfu.edu.cn (Y.W.); liulin2385@bjfu.edu.cn (L.L.); gaoyanan0302@bjfu.edu.cn (Y.G.); flame1@bjfu.edu.cn (Z.G.)

* Correspondence: zhanglp418@163.com

Abstract: In this study, coal fly ash was functionalized, using a simple one-step process (loading with Al^{3+} and sulfonation), to yield a solid acid catalyst (S/Al-CFA) with strong acid sites. The catalyst was then used to produce furfural from xylose in a biphasic system ($H_2O_{(NaCl)}/$ tetrahydrofuran). The furfural yield reached 82% at 180 °C–60 min with catalyst/xylose ratio of 0.2:1.0 (w/w). With the reaction completed, all of the components could be effectively separated, and the furfural was 97.6% pure. The cycle and regeneration of the catalyst were evaluated, and the catalyst deactivation mechanism was investigated.

Keywords: furfural; xylose; functionalized coal fly ash; biphasic system; recyclable



Citation: Li, M.; Wang, Y.; Liu, L.; Gao, Y.; Gao, Z.; Zhang, L. Functionalized Coal Fly Ash Is an Efficient Catalyst for Synthesizing Furfural from Xylose at a Low Catalyst Load. *Catalysts* **2023**, *13*, 1492. <https://doi.org/10.3390/catal13121492>

Academic Editor: Gartzzen Lopez

Received: 11 October 2023

Revised: 27 November 2023

Accepted: 30 November 2023

Published: 5 December 2023



Copyright: © 2023 by the authors. Licensee MDPI, Basel, Switzerland. This article is an open access article distributed under the terms and conditions of the Creative Commons Attribution (CC BY) license (<https://creativecommons.org/licenses/by/4.0/>).

1. Introduction

Furfural, a valuable biomass-derived platform chemical, plays a vital role in the seamless transition from the present fossil fuel-centered economy toward a carbon-neutral future [1–3]. The use of solid acid catalysts is superior to that of mineral acids in furfural production systems, and the use of biphasic systems is superior to that of single-phase systems; thus, biphasic systems using solid acids have been studied extensively [4–6]. However, there are important drawbacks to the currently available biphasic systems, including the following: the catalysts are complicated to prepare, high catalyst doses (sometimes exceeding the xylose dose) are needed, and the components of the system are difficult to separate and recover after the reaction has reached completion [5,7–10].

Various solid acid catalysts for producing furfural have been synthesized. These include Cr-deAl-Y [11], Sn-Beta [12], γ - Al_2O_3 [13], Nb_2O_5 [14], MSPFR [15], $Cl_{0.3}$ -SR [16], $SO_4^{2-}/$ Sn-TRP [17], $SO_4^{2-}/$ SnO₂-Al₂O₃-CFA [9]. In contrast to other solid acid catalysts, coal fly ash (CFA) is a solid waste from coal-burning power plants, and there is great interest in developing CFA-based catalysts because CFA is very thermally stable, cheap, and possible to functionalize [18,19]. However, CFA-based catalysts, like other solid acid catalysts, require relatively high catalyst: xylose ratios (w/w), as shown in Table 1. Moreover, preparing solid acids consumes a lot of energy and comes with safety risks, due to the strongly corrosive acids (e.g., sulfuric acid or chlorosulfonic acid), elevated temperatures (for calcination), and long preparation times used [20–23]. Many solid acid catalysts are poorly reusable [24]. Therefore, choosing a simple and effective method through which to modify a catalyst for converting xylose into furfural is important.

Table 1. Solid acid catalysts for converting xylose into furfural.

Catalyst	Reaction Condition			Yield (Furfural)	Ref
	Solvent	Temperature—Time	Xylose:Catalyst Ratio		
SO ₄ ²⁻ /SnO ₂ -Al ₂ O ₃ -CFA	Water/toluene	180 °C–30 min	1.06	84.7	[9]
Sulfuric acid-treated CFA	Water/toluene	170 °C–210 min	0.67	68	[23]
S-IRCC	Water/MIBK	190 °C–60 min	1	73.64	[24]
SO ₄ ²⁻ /Sn-TRP	Water/toluene	170 °C–180 min	2	82.79	[17]
SO ₄ ²⁻ /SnO ₂ -SSXR	ChCl-MAA/toluene	180 °C–15 min	0.53	82.6	[5]
Sn-MMT	SBP/NaCl-DMSO	180 °C–30 min	5	76.79	[25]
γ-Al ₂ O ₃	Water/toluene	150 °C–60 min	0.71	23	[13]
Nb ₂ O ₅	Water/toluene	120 °C–180 min	1.34	53.23	[14]
Cl _{0.3} -S-R	water/1,4-dioxane	190 °C–80 min	1	38.1	[16]
S/Al-CFA	Water/THF	180 °C–60 min	0.2	82	This work

Modifying a catalyst, by loading it with metal ions that act as Lewis acid sites and sulfonating it to provide Brønsted acid sites, can typically improve catalytic performance [17]. Specifically, Al³⁺ forms a well-activated metal center as an especially efficient Lewis acid site for facilitating xylose to produce furfural [13,26]. Sulfonation, using sulfamic acid as a sulfonating agent and NaNO₂ as a diazotizing agent, is a simple process that produces relatively little hazardous waste [27,28]. Moreover, solid acid catalysts based on sulfonic acid provide a high degree of activity for furfural production, can be reused effectively, and are thermally stable [24,29]. Treating CFA with citric acid before modification can improve CFA activity and remove impurities [30,31].

The chemical stability of furfural is poor, and it is sensitive to solvent environmental changes, so choosing a proper solvent system is crucial for furfural synthesis [32]. Biphasic systems, consisting of water and organic solvents, offer marked advantages over expensive ionic liquids and inefficient pure water systems, including being very efficient and cheap, and allowing for the components to be separated easily when the reaction is complete [33]. Higher furfural yields have been found using polar aprotic solvents than with other solvents [34,35]. A markedly higher furfural yield has been found using tetrahydrofuran (THF) than using other polar aprotic solvents [36]. The boiling point of THF (66 °C) is much lower than the boiling point of furfural (162 °C), so less energy is consumed when separating furfural from THF than from solvents with higher boiling points. NaCl is one of the cheapest and most effective salts for promoting separation of the H₂O and THF phases, improving THF extraction, and slowing down furfural degradation [11,12]. NaCl also promotes the dehydration of xylose and, thus, increases the furfural yield [29].

In this work, we prepared a solid acid catalyst (S/Al-CFA) with strong acid sites by subjecting CFA to a simple one-step process through which to simultaneously load the CFA with aluminum ions and sulfonate the CFA. The S/Al-CFA was used to catalyze the preparation of furfural from xylose in an H₂O(NaCl)/THF two-phase system. The reaction conditions were optimized, and a furfural yield of 82% was obtained at a low catalyst:xylose ratio (*w/w*). The components of the reaction system were able to be effectively recovered. The recovered solid acid catalyst maintained excellent performance for five cycles. The furfural obtained after separation was 97.6% pure, and the furfural concentration in the THF was only 0.6%. The fresh and recovered catalysts were characterized to determine

why the catalyst became deactivated. Finally, the ability of the catalytic system to produce furfural from corn cob hydrolysate, using optimal conditions, was assessed.

2. Results and Discussion

2.1. Characterization of Catalysts

SEM images of the CFA and S-CFA-Al are shown in Figure S1. The CFA (A-1 and A-2) consisted of spherical particles of different sizes that were mainly composed of an amorphous glass phase with smooth surfaces. In S/Al-CFA (B-1, B-2), the smooth surface was destroyed to form small spherical particles with relatively rough and wrinkled surfaces. Combined with the BET results (Table 2), the S/Al-CFA surface area ($10.805 \text{ m}^2/\text{g}$) was about eight times higher than the CFA surface area ($1.413 \text{ m}^2/\text{g}$), meaning the S/Al-CFA would have had more adsorption sites [37].

Table 2. Characteristics of the catalysts.

Catalyst	S_{BET} (m^2/g)	D (nm)	V_{Meso} (cm^3/g)	Total Acid $\mu\text{mol}/\text{g}$
CFA	1.413	3.823	0.012	356
C-CFA	13.229	4.826	0.037	-
S/Al-CFA	10.805	4.404	0.035	2390
R-S/Al-CFA	7.244	3.905	0.023	1849

S_{BET} : The specific surface area, measured using the BET method. D: The pore sizes, measured using the BJH adsorption method. V_{Meso} : The mesopore volumes, measured using the BJH adsorption method.

The element contents and distributions were analyzed using an energy-dispersive detector attached to the SEM to verify that loading with Al and sulfonation had been successful during the S/Al-CFA preparation process. As shown in Table S2, the S and Al contents of the CFA were 0.14 wt% and 1.35 wt%, respectively, and the S and Al contents of the S/Al-CFA were 7.85 wt% and 8.96 wt%, respectively, indicating that S and Al were successfully introduced into the CFA. As shown in Figure S1, the energy-dispersive spectroscopy maps of the S/Al-CFA indicated that Al and S were uniformly spread across the CFA surfaces.

The FT-IR and Xps spectra of catalysts are shown in Figure 1a,b. In the FT-IR spectra, the bands at 455 , 559 , and 1092 cm^{-1} in CFA and S/Al-CFA were attributed to Si-O-Si, O-Si-O, and Si-O-Al stretching, respectively [38]. The FT-IR spectrum of S/Al-CFA in the 3468 cm^{-1} band was the Al-OH stretching vibrations peak. This indicates that Al^{3+} was successfully loaded onto the CFA. The width of the band represented the hydrogen bonding between the hydroxyl groups, indicating that the treatment increased the number of hydroxyl groups and, therefore, the Brønsted acid acidity [23,38]. In S/Al-CFA, the $-\text{SO}_3\text{H}$ group could be identified in the 1037 and 1009 cm^{-1} bands [39]. In addition, the XPS spectrum of S/Al-CFA contained a single S2p peak, indicating that all of the S was present as SO_3H [22].

The XRD pattern of CFA (Figure S2) contained a broad diffraction peak at $15\text{--}34^\circ$, which was mainly caused by vitreous, SiO_2 , and $\text{SiO}_2\text{--Al}_2\text{O}_3$ areas in the CFA. These areas would have given the CFA relatively strong hydrophilicity and surface activity, as well as good sorption ability [9]. The XRD spectrum of C-CFA contained the same peaks as the CFA spectrum, indicating that the citric acid treatment did not affect the crystal structure of the CFA. The citric acid preferentially removed nonstructural aluminum from the CFA to adjust the pore structure [40,41]. No additional characteristic peaks were found after Al loading and sulfonation. The mesopore volume and specific surface area were lower for the S/Al-CFA than for the C-CFA (Table 2). This, and the element map of S/Al-CFA, indicates that the catalyst preparation procedure caused the metal ions and sulfonic acid groups to be uniformly spread across the CFA surfaces.

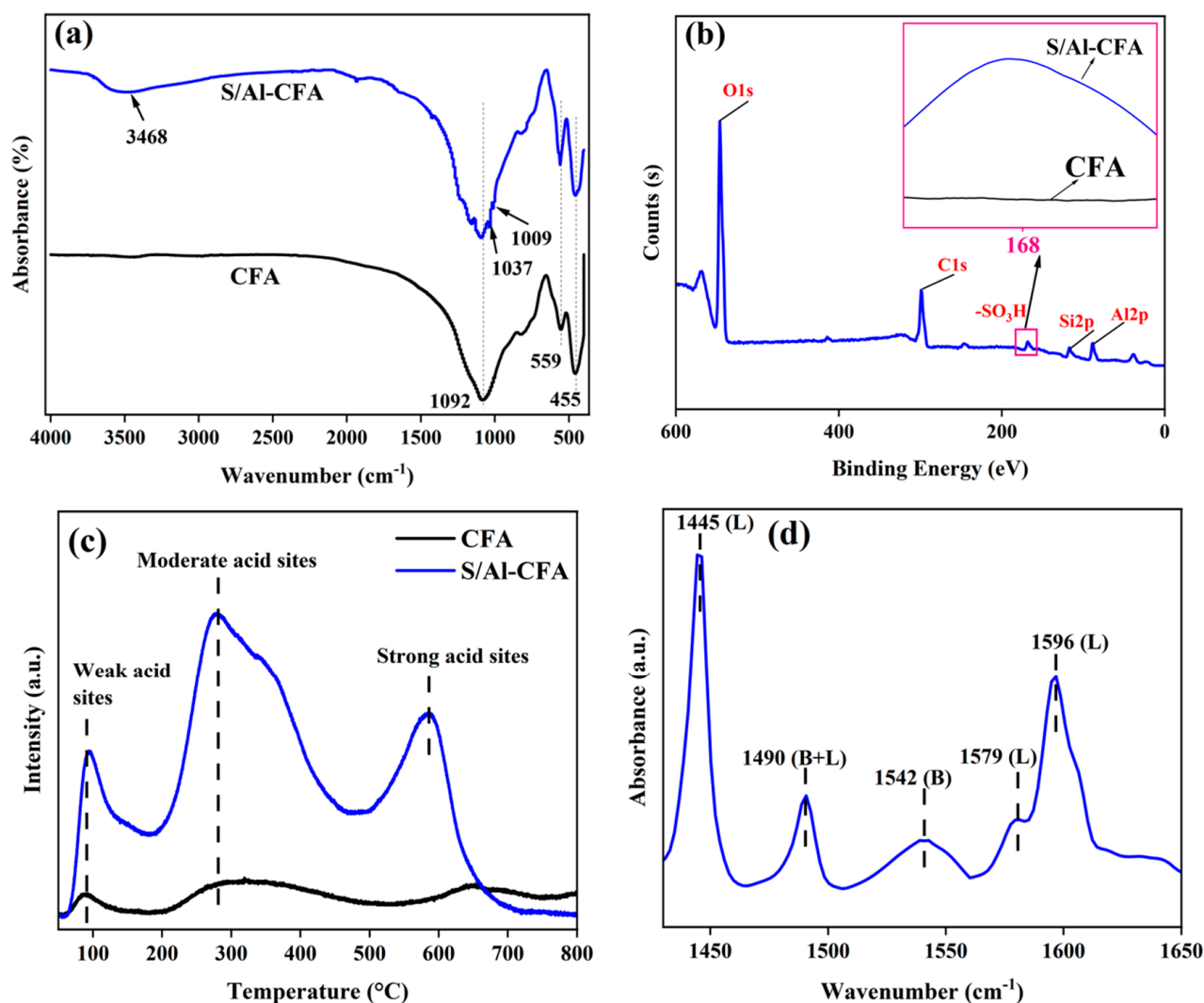


Figure 1. Characterization of catalysts. (a) FT-IR, (b) Xps, (c) NH₃-TPD, and (d) Py-FTIR.

As shown in Figure S3, the CFA was thermally stable at <400 °C. The modified catalyst remained thermally stable, allowing the S/Al-CFA to perform very well for at least five cycles.

The N₂ adsorption–desorption isotherms for the catalysts are shown in Figure S4. According to IUPAC nomenclature, the BET isotherms of catalysts were all of type IV, and the hysteresis loops were type H3 [23]. This suggested that the materials were mesoporous, with slit-shaped or panel-shaped pores [42]. In Table 2, the N₂ adsorption–desorption analysis results of the catalysts are summarized. The pore volume and specific surface area were markedly higher for the C-CFA than for the CFA because the citric acid removed some metals and impurities from the CFA. The mesopore volume and specific surface area were lower for the S/Al-CFA than for the C-CFA, indicating that –SO₃H and Al³⁺ were uniformly distributed through the mesopores. The specific surface area, pore size and mesopore volume for the S/Al-CFA were higher than for the CFA, meaning that more catalytically active sites were exposed on the S/Al-CFA, promoting the production of furfural [23]. The furfural and xylose molecular radii were 0.68 and 0.86 nm, respectively [17]. The mean S/Al-CFA pore diameter was 4.404 nm, indicating that furfural may readily diffuse out of S/Al-CFA pores, and that xylose may readily reach the acidic sites in S/Al-CFA pores.

NH₃-TPD was used to evaluate the acid strength and total acid of the catalyst. NH₃ desorption at 100–200, 200–400, and 400–800 °C indicated weakly acidic, moderately acidic, and strongly acidic sites, respectively [43]. As shown in Figure 1c, the S/Al-CFA had

moderately and strongly acidic sites (at 277 and 585 °C, respectively). The CFA did not contain strongly acidic sites. As shown in Table 2, the total acid content was higher for the S/Al-CFA than for the CFA because of the $-\text{SO}_3\text{H}$ and Al^{3+} present in the S/Al-CFA. In Table S3, the amounts of weak, moderate, and strong acids were listed for the CFA and S-Al-CFA catalysts, respectively. Py-FTIR was performed to distinguish the acid types. As shown in Figure 1d, the S/Al-CFA contained Brønsted and Lewis acid sites (B and L acid). The bands at 1445, 1490, 1542, 1579, and 1596 cm^{-1} were attributed to L, B; L, B, L; and L acid sites, respectively [44].

2.2. Effects of Using Modified CFA on the Furfural Yield

As shown in Figure 2, furfural yields from xylose when the modified CFA catalysts were used increased in the order CFA < Fe-CFA < Cr-CFA < Al-CFA < S/Fe-CFA < S/Cr-CFA < S/Al-CFA. The actual yields are shown in Table S1. The highest furfural yield (72%) was given by the solid acidic catalyst S/Al-CFA. The solid acid catalysts, with simultaneous Brønsted and Lewis acids, catalyzed furfural production from xylose well, since the Brønsted and Lewis acids could participate synergistically in furfural production [5,21,45,46]. Therefore, co-modifying sulfonation and loaded metal ions markedly improved the catalytic activity. This could be explained by the two-step reaction mechanism proposed by Suzuki et al. [35]. Tests were performed using catalysts prepared using FeCl_3 , CrCl_3 , and AlCl_3 at various concentrations to assess the effects on the furfural yield. S/Al-CFA had the highest activity when the AlCl_3 concentration was 15 mM, which gave a furfural yield of 72%. More oxidation of xylose to CO_2 occurred in the presence of Cr^{3+} and Fe^{3+} than in the presence of Al^{3+} , resulting in lower furfural yields with the existence of Cr^{3+} and Fe^{3+} than with Al^{3+} [47]. In Scheme S1, a possible reaction pathway for S-Al-CFA catalyzed xylose to furfural is described.

2.3. Reaction System Determination

The NaCl concentration affected the furfural yield. As shown in Figure 3a, 22% lower furfural yields were gained without the added NaCl. Increasing the NaCl concentration from 0 to 250 g/L increased the furfural yield, from 22% to 72%. Adding NaCl to an H_2O –THF system would have markedly increased the furfural concentration in the THF by affecting the intramolecular binding of the liquid phase constituents and making H_2O and THF less miscible [12]. NaCl would also have increased the furfural concentration by increasing the reaction rate [6,48]. The maximum furfural yield was 72% when the NaCl concentration was 250 g/L. Increasing the NaCl concentration further caused the furfural yield to decrease, to 68%, because the high Cl^- concentration would have inhibited furfural formation [24].

After the optimal NaCl concentration had been determined, the effect of the THF dose on the furfural yield was assessed. The highest furfural yield was 72%, which was achieved at a THF dose of 100 mL (H_2O : THF ratio 1:2 (v/v)), as shown in Figure 3b. This indicates that a certain THF dose increased the furfural yield. An excess of the aqueous phase would have weakened the reactivity of the acidic catalyst, and an excess of the organic phase would have led to the formation of unwanted humins [49,50]. THF used as an extractant phase can transfer furfural formed in the aqueous solution in real time and, therefore, shift the reaction equilibrium in the positive direction and prevent secondary loss reactions, meaning that the furfural that is produced is protected in the THF [51].

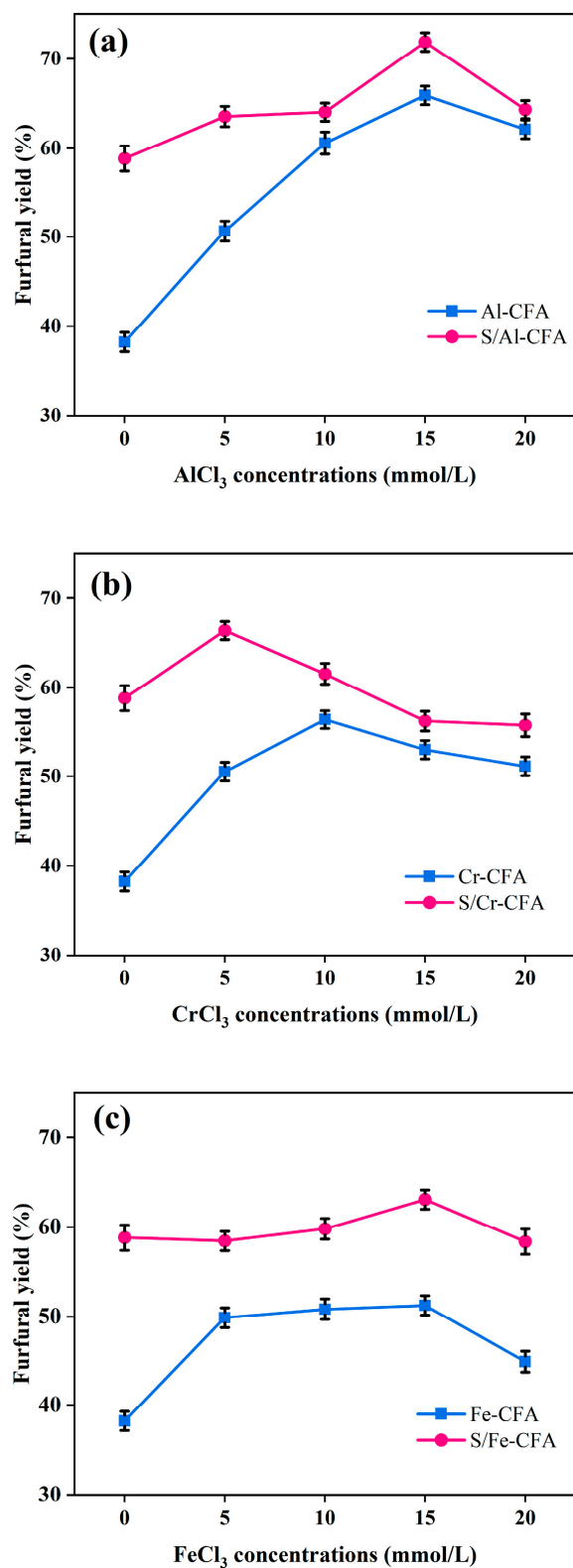


Figure 2. The effects of different metal ion concentrations during catalyst preparation on the catalyst performance under the same reaction conditions (180 °C, 30 min, catalyst: xylose ratio 0.2:1.0 (*w/w*), THF: H₂O(NaCl) ratio 2:1 (*v/v*), 250 (g NaCl)/L). (a) Effect of the AlCl₃ concentration on the modified CFA performance. (b) Effect of the CrCl₃ concentration on the modified CFA performance. (c) Effect of the FeCl₃ concentration on the modified CFA performance.

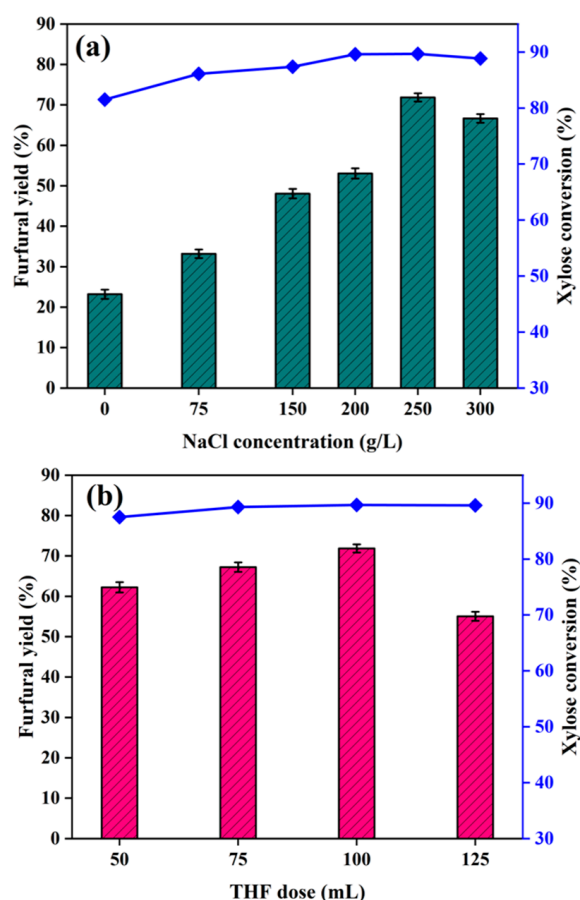


Figure 3. Effects of NaCl concentration and THF dose on the xylose conversion rate and furfural yield. Reaction conditions: (a) 30 min, 180 °C, catalyst: xylose ratio 0.2:1.0 (*w/w*), H₂O: THF ratio 1:2 (*v/v*) and (b) catalyst: xylose ratio 0.2:1.0 (*w/w*), 50 mL of 250 g/L NaCl.

2.4. Optimizing the Reaction Conditions

The reaction conditions were optimized, and the results are shown in Figure 4a,b. At the beginning of the reaction, the furfural yield and xylose conversion rate grew as the time and temperature increased. Lower temperatures and times did not provide enough energy to facilitate xylose conversion [11,52]. Initially, the furfural yield increased with increasing reaction time or reaction temperature, and the maximum furfural yield, of 82%, was achieved at 180 °C and 60 min. Subsequently, increasing the reaction temperature or extending the reaction time decreased the furfural yield (to 75% at 75 min, or 77% at 190 °C). This was because the intense systemic energy exacerbated unwanted side reactions [25]. Various byproducts could be deposited on the active sites of the catalyst, thus decreasing the catalytic activity and the furfural synthesis efficiency [9].

Figure 4c shows the effect of the S/Al-CFA dose on the furfural yield. When no catalyst was added, only 55% and 26% for xylose conversion and furfural yield were obtained, respectively. Adding S/Al-CFA dramatically improved the xylose conversion rate and furfural yield. A catalyst dose of 0.1 g gave a furfural yield of 76%. Moreover, adding the catalyst gave a xylose conversion rate of >90% in all of the tests, indicating that the S/Al-CFA could fully bond xylose and facilitate xylose conversion. The maximum furfural yield was 82%, and this was achieved at a S/Al-CFA dose of only 0.2 g (catalyst: xylose ratio 0.2 (*w/w*)). Using a lower catalyst dose will also be cheaper; therefore, the S/Al-CFA catalyst has a clear advantage over most catalysts, which need to be used at high doses. Increasing the S/Al-CFA dose further caused the furfural yield to decrease, to 68%, because the S/Al-CFA provided excess acidic sites that catalyzed side reactions of furfural [28].

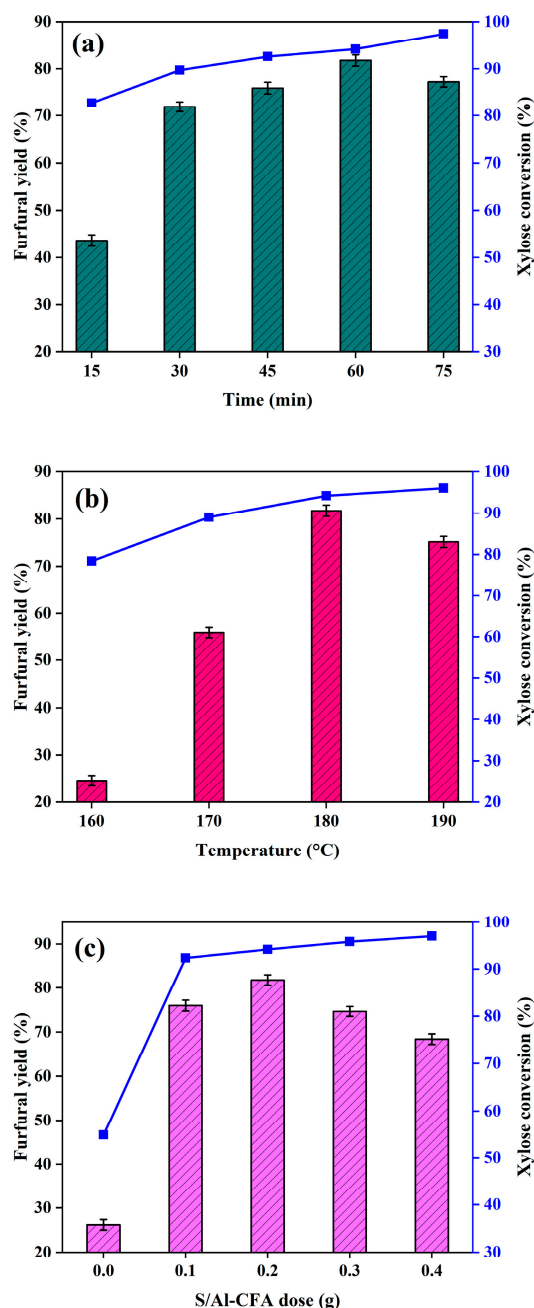


Figure 4. Effects of reaction time, reaction temperature, and S/Al-CFA dose on the xylose conversion rate and furfural yield. Reaction conditions: (a) 180 °C, H₂O: THF ratio 1:2 (*v/v*), catalyst: xylose ratio 0.2:1.0 (*w/w*), 250 g/L NaCl; (b) 60 min, H₂O: THF ratio 1:2 (*v/v*), catalyst: xylose ratio 0.2:1.0 (*w/w*), 250 g/L NaCl; and (c) 60 min, 180 °C, H₂O: THF ratio 1:2 (*v/v*), xylose dose 1.0 g, 250 g/L NaCl.

2.5. Separation and Recovery of Catalytic System Components

Furfural production can be made more economically efficient if the catalytic system components can be efficiently separated and recovered. The feasibility of recovering all of the components was investigated. As shown in Figure 5, the solvent system and catalyst were first separated through filtration, and then the recovered S/Al-CFA catalyst was used in another reaction. The H₂O_(NaCl) and THF phases were separated in a separatory funnel. The different boiling points of THF and furfural allowed THF and furfural to be separated through reduced-pressure distillation. The samples were analyzed using HPLC. At 40–60 °C, the furfural concentration in the collected THF was 0.6%. At 60–85 °C, the collected furfural was 97.6% pure. The NaCl in the water was recovered by evaporating

the water. All of the components were able to be recovered. The results indicated that the $\text{H}_2\text{O}(\text{NaCl})\text{-THF}$ catalytic system containing S/Al-CFA was both efficient and recyclable and has great potential for practical use.

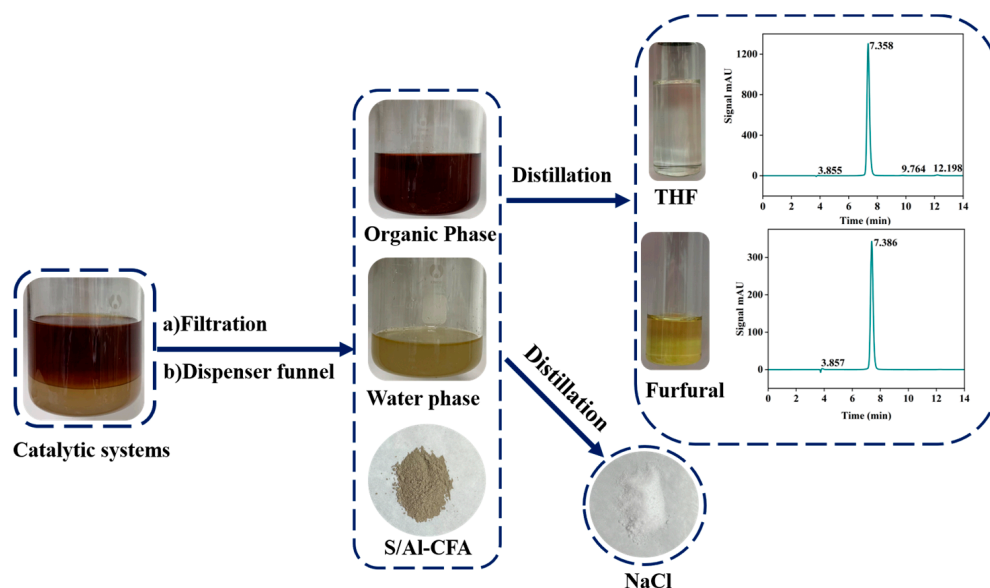


Figure 5. Separation and recovery of the catalytic system components.

2.6. Catalyst Recyclability

Recycling a catalyst can improve the sustainability of the process being performed. The separated S/Al-CFA was washed with deionized water and ethanol, and dried at 110 °C for 5 h before reuse. As shown in Figure 6, the first-cycle yield of furfural was 76%, which was only 6% lower than the yield using the fresh catalyst. After four cycles, the furfural yield still reached 75%.

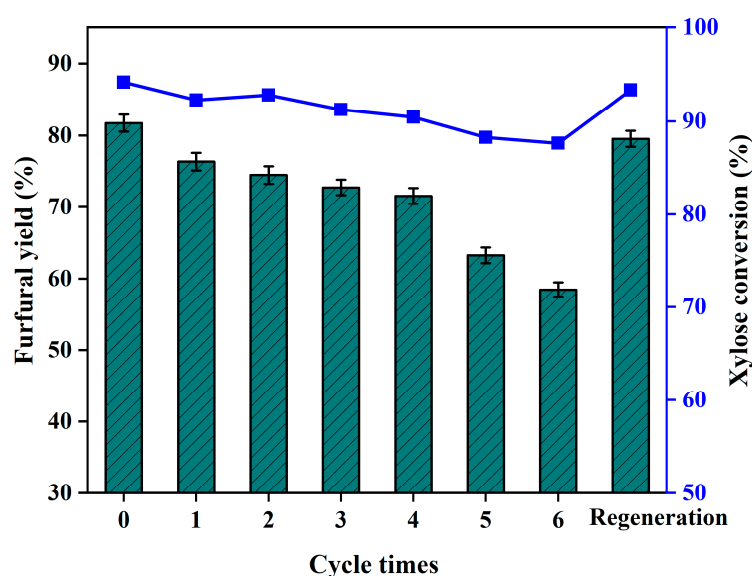


Figure 6. Xylose conversion rates and furfural yields for recycled S/Al-CFA. Reaction conditions: 180 °C, 60 min, catalyst: xylose ratio 0.2:1.0 (*w/w*), H_2O : THF ratio 1:2 (*v/v*), 250 g/L NaCl.

The catalyst that had been recovered six times (R-S/Al-CFA) was subjected to FT-IR spectroscopy, NH_3 -TPD, and BET analysis. As shown in Figure 7, the R-S/Al-CFA FT-IR spectrum at 1547 and 1577 cm^{-1} contained new weak bands, which were attributed to C=C bonds [53]. This may indicate the deposition or adsorption of humins produced

during reactions on the S/Al-CFA. As shown in Table 2, the specific surface area, pore size, pore volume, and total acidity were markedly lower for the R-S/Al-CFA than for the S/Al-CFA, and strong acid sites had been lost during use (Figure 7). This loss may have been responsible for the marked decrease in furfural yield.

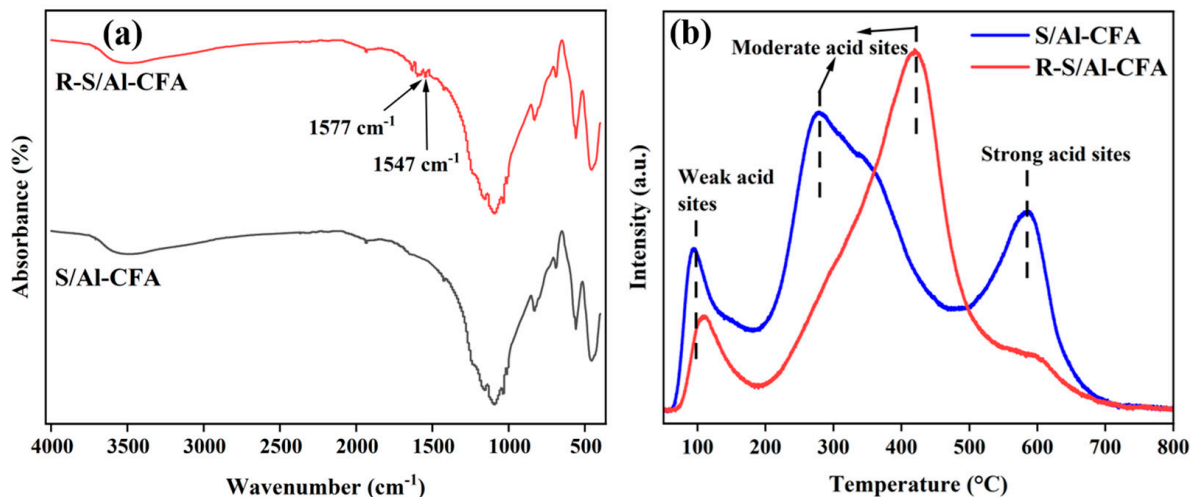


Figure 7. Characterization of the catalyst before and after cycling. (a) FT-IR and (b) NH_3 -TPD.

The regeneration method for R-S/Al-CFA was described in the second paragraph of Section 3.2. Regenerated R-S/Al-CFA was used to catalyze xylose conversion to furfural. The furfural yield was only 2% lower when using regenerated R-S/Al-CFA than when using fresh S/Al-CFA. This indicates that used S/Al-CFA could be reactivated using the regeneration method.

2.7. S/Al-CFA Catalysis of Corncob Hydrolysates

Furfural is usually produced commercially, using corncobs, oat hulls, and cottonseed hulls as raw materials [54,55]. These types of biomass contain more complex components (e.g., cellulose, hemicellulose, lignin, and mineral salts) than xylose. These components may yield complex products (e.g., hydrolyzed cellulose sugars and hydrolyzed lignin phenols) during hydrolysis, and these products may affect furfural production [11,39].

We used the described method in Section 3.4 to prepare a xylose-rich hydrolysate. The xylose concentration in the xylose-rich hydrolysate was 60 g/L. Under optimal conditions, the furfural yield was 80%, and the xylose conversion rate was 100%. Impurities in the corncob hydrolysate slightly decreased the catalytic activity, but ideal catalytic results were still found. This indicates that the S/Al-CFA offers promise for practical use in producing furfural from corncob hydrolysates.

3. Materials and Methods

3.1. Materials

Corncobs from Hebei Province, China, were washed with water, dried at 50 °C to a constant weight, and then crushed to pass through a 60–80 mesh sieve. CFA (5000 mesh) was purchased from Henan Hengyuan New Material Co. (Henan, China). $\text{AlCl}_3 \cdot 6\text{H}_2\text{O}$, citric acid (CA, analytical reagent grade (AR)), $\text{CrCl}_3 \cdot 6\text{H}_2\text{O}$, $\text{FeCl}_3 \cdot 6\text{H}_2\text{O}$, ethanol (AR), maleic acid (AR), NaCl (AR), NaNO_2 (AR), sulfanilic acid (AR), THF (AR), and xylose (98%) were all obtained from Shanghai Maclin Biochemical Technology Co. (Shanghai, China). All reagents were used without further purification.

3.2. Preparation of Modified CFA Solid Acid Catalysts

First, 4 g CFA was added to 100 mL of 0.8 M CA solution, and then the mixture was maintained in a water bath at 80 °C for 5 h with stirring. The mixture was then filtered

with a reduced pressure filtration operation, the collected solid was washed until the wash water was neutral, and then the solid was dried at 110 °C for 5 h. Activated CFA (C-CFA) was obtained.

Thereafter, 2 g of C-CFA and 8 g of sulfanilic acid were added to 100 mL of a specific concentration (0, 5, 10, 15, 20 mmol/L) of AlCl₃ (FeCl₃, CrCl₃) solution. The mixture was stirred in a water bath at 80 °C for 40 min, then 4 g of NaNO₂ was added, and the mixture was stirred for another 10 h at 80 °C in the water bath. Modified CFA (S/Al-CFA, S/Fe-CFA, S/Cr-CFA) was washed with deionized water until the wash water was neutral, and it was dried at 110 °C for 5 h. The solid acid catalyst S/Al-CFA (S/Fe-CFA, S/Cr-CFA) was obtained. Other solid acids were prepared accordingly, including Al-CFA, Fe-CFA, Cr-CFA, and S/CFA.

3.3. Catalyst Characterization

Scanning electron microscopy images, energy-dispersive spectra, and relative element maps of the catalysts were acquired using a TESCAN MIRA LMS scanning electron microscope (TESCAN, Brno, Czech Republic) equipped with an Xplore 30 energy-dispersive detector (Oxford Instruments, Abingdon, UK). Fourier transform infrared (FT-IR) spectra of the catalysts were acquired using a Nicolet iS20 instrument (Thermo Fisher Scientific, Waltham, MA, USA) using KBr disks. X-ray photoelectron spectroscopy (XPS) analysis was tested on a Thermo Scientific K-Alpha spectrometer. The crystal structures of the catalysts were determined with X-ray diffractometry (XRD) using a D/MAX-2600 instrument (Rigaku, Tokyo, Japan). Thermogravimetric (TG) analysis was performed using a TG 209 F3 instrument (Netzsch, Selb, Germany). The Brunauer–Emmett–Teller (BET) surface area and pore structure of the samples were analyzed with N₂ adsorption–desorption analysis. The acidic sites were identified and the total acidities of the catalysts were determined through temperature-programmed NH₃ (NH₃-TPD) desorption using a MicrotracBEL Cat II instrument (MicrotracBEL, Osaka, Japan). Pyridine adsorption infrared spectroscopy (Py-FTIR) analysis was performed on a Tensor 27 instrument to detect catalyst Brønsted and Lewis acid types.

3.4. Production of Xylose-Rich Hydrolysate from Corncobs

In a 500 mL Teflon-lined autoclave reactor (China Wuzhou Dingchuang Beijing Technology Co., Beijing, China), 100 mL of 0.15 M maleic acid solution and 5 g of corncob were mixed thoroughly. The reactor was heated to 140 °C for 1 h, and then cooled to 30 °C using circulating cooling water. The hydrolysis solution was obtained through vacuum filtration. The hydrolysate was concentrated with a rotary evaporator to obtain a xylose-rich hydrolysate with which to prepare furfural.

Xylose-oligosaccharides were completely hydrolyzed by subjecting the concentrated hydrolysate to hydrolysis again, using 4% H₂SO₄ at 121 °C for 60 min. The xylose concentration obtained here was used as the value of the moles for xylose units in the corncob.

3.5. Catalytic Tests

Furfural was produced by treating xylose or xylose-rich hydrolysate in a 500 mL quartz-lined autoclave with mechanical stirring at 300 rpm. In a typical test, xylose or xylose-rich hydrolysate, solid acidic catalysts, NaCl solution or NaCl, and THF were added to the autoclave, which was then sealed, and N₂ was introduced to remove the air. The reactor was heated to the desired temperature, which was maintained for a specific duration. Circulating cooling water was then passed through the reactor to cool the contents to 40 °C. The mixture was filtered and the aqueous and THF phases were analyzed using high-performance liquid chromatography (HPLC). To ensure the reliability of the experimental data, each experiment was repeated three times.

3.6. Product Analysis

The furfural concentration was determined with high-performance liquid chromatography using a TC-C18 column (Agilent Technologies, Santa Clara, CA, USA) and a 15/85 (*v/v*) acetonitrile/water mixture as the mobile phase at a flow rate of 1 mL/min. The xylose concentration was determined with high-performance liquid chromatography using an Aminex HPX-87H column (Bio-Rad Laboratories, Hercules, CA, USA), using 5 mmol/L H₂SO₄ as the mobile phase at a flow rate of 0.6 mL/min. The detector used was a refractive index detector. The xylose conversion and furfural yield were calculated using the following formulae:

$$\text{Xylose conversion} = \frac{\text{moles of xylose reacting}}{\text{moles of xylose starting}} \times 100\% \quad (1)$$

$$\text{Furfural yield from xylose} = \frac{\text{moles of furfural produced}}{\text{moles of xylose put into the reactor}} \times 100\% \quad (2)$$

4. Conclusions

The solid acid catalyst S/Al-CFA was prepared using a simple one-step process, using AlCl₃ and sulfanilic acid/NaNO₂. The S/Al-CFA had stronger acid sites, a better developed pore structure, and a markedly higher total acid content than the CFA. The furfural yield at a catalyst: xylose ratio of 0.2 (*w/w*) was 82%. All components of the catalytic system were able to be separated efficiently. The furfural product was 97.6% pure, and the furfural concentration in the THF was only 0.6%. When the catalyst was used over four cycles, the furfural yield remained >72%. Leaching of acidic sites and pore collapse were important factors in the deterioration of the catalytic properties of the S/Al-CFA. The recycled S/Al-CFA was able to be regenerated, and the furfural yield when the regenerated S/Al-CFA was used was 80%, which was similar to the furfural yield using fresh S/Al-CFA. A furfural yield of 80% was found when the S/Al-CFA was used to catalyze the reaction using corncob hydrolysate. In conclusion, a functional catalyst with strong activity for producing furfural from xylose was synthesized using CFA as a substrate, which provides an attractive avenue for the recycling and high value-added utilization of CFA.

Supplementary Materials: The following supporting information can be downloaded at: <https://www.mdpi.com/article/10.3390/catal13121492/s1>, Scheme S1: Possible reaction pathways for furfural formation from xylose catalyzed by S-Al-CFA; Figure S1: SEM images of the CFA (A-1 and B-1) and the S/Al-CFA (A-2 and B-2). Element maps of Al and S in the S/Al-CFA (C and D); Figure S2: XRD patterns of the CFA, C-CFA, and S/Al-CFA; Figure S3: TG results for the CFA and S/Al-CFA; Figure S4: N₂ adsorption–desorption isotherms for CFA, C-CFA, and S/Al-CFA; Table S1: The yield of furfural with different modified CFA catalysts; Table S2: Element compositions of the catalysts determined by EDS; Table S3: Comparison of the catalyst performance before and after the cycle.

Author Contributions: Conceptualization, M.L.; Methodology, M.L.; Software, M.L. and Y.G.; Validation, Y.W., L.L. and Y.G.; Formal analysis, M.L. and Z.G.; Investigation, M.L. and Y.W.; Data curation, L.L.; Writing—original draft, M.L.; Writing—review & editing, M.L., Z.G. and L.Z.; Supervision, L.Z.; Funding acquisition, L.Z. All authors have read and agreed to the published version of the manuscript.

Funding: This research was supported by Ministry of Science and Technology of the People's Republic of China (2019YFB1503803-01-05).

Data Availability Statement: Data is contained within the article or supplementary material.

Conflicts of Interest: The authors declare no conflict of interest.

References

1. Jaswal, A.; Singh, P.P.; Mondal, T. Furfural—A versatile, biomass-derived platform chemical for the production of renewable chemicals. *Green Chem.* **2021**, *24*, 510–551. [[CrossRef](#)]
2. Zhou, Q.; Liu, Z.; Wu, T.Y.; Zhang, L. Furfural from pyrolysis of agroforestry waste: Critical factors for utilisation of C5 and C6 sugars. *Renew. Sustain. Energy Rev.* **2023**, *176*, 113194. [[CrossRef](#)]
3. Mariscal, R.; Maireles-Torres, P.; Ojeda, M.; Sádaba, I.; López Granados, M. Furfural: A renewable and versatile platform molecule for the synthesis of chemicals and fuels. *Energy Environ. Sci.* **2016**, *9*, 1144–1189. [[CrossRef](#)]
4. Qing, Q.; Guo, Q.; Zhou, L.; Wan, Y.; Xu, Y.; Ji, H.; Gao, X.; Zhang, Y. Catalytic conversion of corncob and corncob pretreatment hydrolysate to furfural in a biphasic system with addition of sodium chloride. *Bioresour. Technol.* **2016**, *226*, 247–254. [[CrossRef](#)] [[PubMed](#)]
5. Gong, L.; Zha, J.; Pan, L.; Ma, C.; He, Y. Highly efficient conversion of sunflower stalk-hydrolysate to furfural by sunflower stalk residue-derived carbonaceous solid acid in deep eutectic solvent/organic solvent system. *Bioresour. Technol.* **2022**, *351*, 126945. [[CrossRef](#)] [[PubMed](#)]
6. Zhou, N.; Zhang, C.; Cao, Y.; Zhan, J.; Fan, J.; Clark, J.H.; Zhang, S. Conversion of xylose into furfural over MC-SnO_x and NaCl catalysts in a biphasic system. *J. Clean. Prod.* **2021**, *311*, 127780. [[CrossRef](#)]
7. Jernej, S.; Brett, P.; Andrii, K.; Miha, G.; Blaž, L. A review of bio-refining process intensification in catalytic conversion reactions, separations and purifications of hydroxymethylfurfural (HMF) and furfural. *Chem. Eng. J.* **2021**, *429*, 132325.
8. Deng, A.; Lin, Q.; Yan, Y.; Li, H.; Ren, J.; Liu, C.; Sun, R. A feasible process for furfural production from the pre-hydrolysis liquor of corncob via biochar catalysts in a new biphasic system. *Bioresour. Technol.* **2016**, *216*, 754–760. [[CrossRef](#)]
9. Gong, L.; Xu, Z.; Dong, J.; Li, H.; Han, R.; Xu, G.; Ni, Y. Composite coal fly ash solid acid catalyst in synergy with chloride for biphasic preparation of furfural from corn stover hydrolysate. *Bioresour. Technol.* **2019**, *293*, 122065. [[CrossRef](#)]
10. Guo, T.; Li, X.; Liu, X.; Guo, Y.; Wang, Y. Catalytic Transformation of Lignocellulosic Biomass into Arenes, 5-Hydroxymethylfurfural, and Furfural. *ChemSusChem* **2018**, *11*, 2758–2765. [[CrossRef](#)]
11. Ye, W.; Yanan, D.; Tianhao, W.; Mengling, L.; Ying, Z.; Liping, Z. Efficient conversion of xylose to furfural over modified zeolite in the recyclable water/n-butanol system. *Fuel Process. Technol.* **2022**, *237*, 107472.
12. Nikolla, E.; Román-Leshkov, Y.; Moliner, M.; Davis, M.E. “One-Pot” Synthesis of 5-(Hydroxymethyl)furfural from Carbohydrates using Tin-Beta Zeolite. *ACS Catal.* **2011**, *1*, 408–410. [[CrossRef](#)]
13. Fúnez-Núñez, I.; García-Sancho, C.; Cecilia, J.A.; Moreno-Tost, R.; Serrano-Cantador, L.; Maireles-Torres, P. Recovery of pentoses-containing olive stones for their conversion into furfural in the presence of solid acid catalysts. *Process Saf. Environ.* **2020**, *143*, 1–13. [[CrossRef](#)]
14. Gupta, N.K.; Fukuoka, A.; Nakajima, K. Amorphous Nb₂O₅ as a selective and reusable catalyst for furfural production from xylose in biphasic water and toluene. *ACS Catal.* **2017**, *7*, 2430–2436. [[CrossRef](#)]
15. Zhang, T.; Li, W.; An, S.; Huang, F.; Li, X.; Liu, J.; Pei, G.; Liu, Q. Efficient transformation of corn stover to furfural using p-hydroxybenzenesulfonic acid-formaldehyde resin solid acid. *Bioresour. Technol.* **2018**, *264*, 261–267. [[CrossRef](#)] [[PubMed](#)]
16. Tao, Y.; Dong, C.; Wenzhi, L.; Hao, Z. Efficient conversion of corn stover to 5-hydroxymethylfurfural and furfural using a novel acidic resin catalyst in water-1, 4-dioxane system. *Mol. Catal.* **2021**, *515*, 111920.
17. Teng, X.; Si, Z.; Li, S.; Yang, Y.; Wang, Z.; Li, G.; Zhao, J.; Cai, D.; Qin, P. Tin-loaded sulfonated rape pollen for efficient catalytic production of furfural from corn stover. *Ind. Crop. Prod.* **2020**, *151*, 112481. [[CrossRef](#)]
18. Gao, Y.; Jiang, J.; Meng, Y.; Aihemaiti, A.; Ju, T.; Chen, X.; Yan, F. A novel nickel catalyst supported on activated coal fly ash for syngas production via biogas dry reforming. *Renew. Energy* **2020**, *149*, 786–793. [[CrossRef](#)]
19. Peixoto, A.F.; Silva, S.M.; Costa, P.; Santos, A.C.; Valentim, B.; Lázaro-Martínez, J.M.; Freire, C. Acid functionalized coal fly ashes: New solid catalysts for levulinic acid esterification. *Catal. Today* **2019**, *357*, 74–83. [[CrossRef](#)]
20. Jiawei, S.; Ruiying, G.; Yu-Cai, H.; Cuiluan, M. Efficient synthesis of furfural from waste biomasses by sulfonated crab shell-based solid acid in a sustainable approach. *Ind. Crop. Prod.* **2023**, *202*, 116989.
21. Li, X.; Lu, X.; Liang, M.; Xu, R.; Yu, Z.; Duan, B.; Lu, L.; Si, C. Conversion of waste lignocellulose to furfural using sulfonated carbon microspheres as catalyst. *Waste Manag.* **2020**, *108*, 119–126. [[CrossRef](#)] [[PubMed](#)]
22. Wang, Y.; Len, T.; Huang, Y.; Diego Taboada, A.; Boa, A.N.; Ceballos, C.; Delbecq, F.; Mackenzie, G.; Len, C. Sulfonated sporopollenin as an efficient and recyclable heterogeneous catalyst for dehydration of d-Xylose and xylan into furfural. *ACS Sustain. Chem. Eng.* **2016**, *5*, 392–398. [[CrossRef](#)]
23. Chatterjee, A.; Hu, X.; Lam, F.L. Modified coal fly ash waste as an efficient heterogeneous catalyst for dehydration of xylose to furfural in biphasic medium. *Fuel* **2019**, *239*, 726–736. [[CrossRef](#)]
24. Dai, Y.; Yang, S.; Wang, T.; Tang, R.; Wang, Y.; Zhang, L. High conversion of xylose to furfural over corncob residue-based solid acid catalyst in water-methyl isobutyl ketone. *Ind. Crop. Prod.* **2022**, *180*, 114781. [[CrossRef](#)]
25. Li, H.; Ren, J.; Zhong, L.; Sun, R.; Liang, L. Production of furfural from xylose, water-insoluble hemicelluloses and water-soluble fraction of corncob via a tin-loaded montmorillonite solid acid catalyst. *Bioresour. Technol.* **2014**, *176*, 242–248. [[CrossRef](#)] [[PubMed](#)]
26. Li, H.; Wang, X.; Liu, C.; Ren, J.; Zhao, X.; Sun, R.; Wu, A. An efficient pretreatment for the selectively hydrothermal conversion of corncob into furfural: The combined mixed ball milling and ultrasonic pretreatments. *Ind. Crop. Prod.* **2016**, *94*, 721–728. [[CrossRef](#)]

27. Zhang, T.; Li, W.; Jin, Y.; Ou, W. Synthesis of sulfonated chitosan-derived carbon-based catalysts and their applications in the production of 5-hydroxymethylfurfural. *Int. J. Biol. Macromol.* **2020**, *157*, 368–376. [[CrossRef](#)] [[PubMed](#)]
28. Zhang, T.; Li, W.; Xu, Z.; Liu, Q.; Ma, Q.; Jameel, H.; Chang, H.; Ma, L. Catalytic conversion of xylose and corn stalk into furfural over carbon solid acid catalyst in γ -valerolactone. *Bioresour. Technol.* **2016**, *209*, 108–114. [[CrossRef](#)]
29. Xiouras, C.; Radacsi, N.; Sturm, G.; Stefanidis, G.D. Furfural Synthesis from d-Xylose in the Presence of Sodium Chloride: Microwave versus Conventional Heating. *ChemSusChem* **2016**, *9*, 2159–2166. [[CrossRef](#)]
30. Rezaei, H.; Ziaedin Shafaei, S.; Abdollahi, H.; Shahidi, A.; Ghassa, S. A sustainable method for germanium, vanadium and lithium extraction from coal fly ash: Sodium salts roasting and organic acids leaching. *Fuel* **2021**, *312*, 122844. [[CrossRef](#)]
31. Wang, X.; Wang, M.; Zou, D.; Wu, C.; Li, T.; Gao, M.; Liu, S.; Wang, Q.; Shimaoka, T. Comparative study on inorganic Cl removal of municipal solid waste fly ash using different types and concentrations of organic acids. *Chemosphere* **2020**, *261*, 127754. [[CrossRef](#)] [[PubMed](#)]
32. Lee, C.B.T.L.; Wu, T.Y. A review on solvent systems for furfural production from lignocellulosic biomass. *Renew. Sustain. Energy Rev.* **2020**, *137*, 110172. [[CrossRef](#)]
33. Tang, J.; Zhu, L.; Fu, X.; Dai, J.; Guo, X.; Hu, C. Insights into the kinetics and reaction network of aluminum Chloride-Catalyzed conversion of glucose in NaCl-H₂O/THF biphasic system. *ACS Catal.* **2016**, *7*, 256–266. [[CrossRef](#)]
34. Dias, A.; Pillinger, M.; Valente, A. Dehydration of xylose into furfural over micro-mesoporous sulfonic acid catalysts. *J. Catal.* **2005**, *229*, 414–423. [[CrossRef](#)]
35. Choudhary, V.; Pinar, A.B.; Sandler, S.I.; Vlachos, D.G.; Lobo, R.F. Xylose isomerization to xylulose and its dehydration to furfural in aqueous media. *ACS Catal.* **2011**, *1*, 1724–1728. [[CrossRef](#)]
36. Hu, X.; Westerhof, R.J.M.; Dong, D.; Wu, L.; Li, C. Acid-Catalyzed Conversion of Xylose in 20 Solvents: Insight into Interactions of the Solvents with Xylose, Furfural, and the Acid Catalyst. *ACS Sustain. Chem. Eng.* **2014**, *2*, 2562–2575. [[CrossRef](#)]
37. Wang, L.; Huang, X.; Zhang, J.; Wu, F.; Liu, F.; Zhao, H.; Hu, X.; Zhao, X.; Li, J.; Ju, X.; et al. Stabilization of lead in waste water and farmland soil using modified coal fly ash. *J. Clean. Prod.* **2021**, *314*, 127957. [[CrossRef](#)]
38. Cui, R.; Ma, S.; Yang, B.; Li, S.; Pei, T.; Li, J.; Wang, J.; Sun, S.; Mi, C. Simultaneous removal of NO_x and SO₂ with H₂O₂ over silica sulfuric acid catalyst synthesized from fly ash. *Waste Manag.* **2020**, *109*, 65–74. [[CrossRef](#)]
39. Li, W.; Zhu, Y.; Lu, Y.; Liu, Q.; Guan, S.; Chang, H.; Jameel, H.; Ma, L. Enhanced furfural production from raw corn stover employing a novel heterogeneous acid catalyst. *Bioresour. Technol.* **2017**, *245*, 258–265. [[CrossRef](#)]
40. Rui, L.; Qixuan, L.; Junli, R.; Xiaobao, Y.; Yingxiong, W.; Lingzhao, K. Dealuminated H β zeolite for selective conversion of fructose to furfural and formic acid. *Green Energy Environ.* **2022**. [[CrossRef](#)]
41. Wang, B.; Yan, X.; Zhang, X.; Zhang, H.; Li, F. Citric acid-modified beta zeolite for polyoxymethylene dimethyl ethers synthesis: The textural and acidic properties regulation. *Appl. Catal. B Environ.* **2020**, *266*, 118645. [[CrossRef](#)]
42. Sing, K.S.W. Reporting physisorption data for gas/solid systems with special reference to the determination of surface area and porosity (Recommendations 1984). *Pure Appl. Chem.* **1985**, *57*, 603–619. [[CrossRef](#)]
43. Li, Y.; Li, Q.; Zhang, P.; Ma, C.; Xu, J.; He, Y. Catalytic conversion of corncob to furfuryl alcohol in tandem reaction with tin-loaded sulfonated zeolite and NADPH-dependent reductase biocatalyst. *Bioresour. Technol.* **2020**, *320*, 124267. [[CrossRef](#)] [[PubMed](#)]
44. Sun, J.; Zhu, K.; Gao, F.; Wang, C.; Liu, J.; Peden, C.H.F.; Wang, Y. Direct conversion of bio-ethanol to isobutene on nanosized Zn_xZryO_zMixed oxides with balanced acid–base sites. *J. Am. Chem. Soc.* **2011**, *133*, 11096–11099. [[CrossRef](#)] [[PubMed](#)]
45. Weingarten, R.; Tompsett, G.A.; Conner, W.C.; Huber, G.W. Design of solid acid catalysts for aqueous-phase dehydration of carbohydrates: The role of Lewis and Brønsted acid sites. *J. Catal.* **2011**, *279*, 174–182. [[CrossRef](#)]
46. Xu, S.; Pan, D.; Wu, Y.; Song, X.; Gao, L.; Li, W.; Das, L.; Xiao, G. Efficient production of furfural from xylose and wheat straw by bifunctional chromium phosphate catalyst in biphasic systems. *Fuel Process. Technol.* **2018**, *175*, 90–96. [[CrossRef](#)]
47. Lyu, X.; Botte, G.G. Investigation of factors that inhibit furfural production using metal chloride catalysts. *Chem. Eng. J.* **2020**, *403*, 126271. [[CrossRef](#)]
48. Li, Z.; Luo, Y.; Jiang, Z.; Fang, Q.; Hu, C. The promotion effect of NaCl on the conversion of xylose to furfural. *Chin. J. Chem.* **2020**, *38*, 178–184. [[CrossRef](#)]
49. Xinyi, X.; Ying, G.; Liping, Z.; Xian, S.; Han, W.; Hui, G.; Siquan, X. Efficient formation of 5-hydroxymethylfurfural from glucose through H- β zeolite catalyst in the recyclable water-tetrahydrofuran biphasic system. *Catal. Today* **2022**, *404*, 229–236.
50. Mellmer, M.A.; Sener, C.; Gallo, J.M.R.; Luterbacher, J.S.; Alonso, D.M.; Dumesic, J.A. Solvent effects in Acid-Catalyzed biomass conversion reactions. *Angew. Chem.* **2014**, *18*, 2331–2334.
51. Morais, A.R.C.; Bogel-Lukasik, R. Highly efficient and selective CO₂-adjunctive dehydration of xylose to furfural in aqueous media with THF. *Green Chem.* **2016**, *18*, 2331–2334. [[CrossRef](#)]
52. Wang, X.; Liu, Y.; Cui, X.; Xiao, J.; Lin, G.; Chen, Y.; Yang, H.; Chen, H. Production of furfural and levoglucosan from typical agricultural wastes via pyrolysis coupled with hydrothermal conversion: Influence of temperature and raw materials. *Waste Manag.* **2020**, *114*, 43–52. [[CrossRef](#)] [[PubMed](#)]
53. Cheng, Z.; Everhart, J.L.; Tsilomelekis, G.; Nikolakis, V.; Saha, B.; Vlachos, D.G. Structural analysis of humins formed in the Brønsted acid catalyzed dehydration of fructose. *Green Chem.* **2018**, *20*, 997–1006. [[CrossRef](#)]

54. Alonso, D.M.; Wettstein, S.G.; Mellmer, M.A.; Gurbuz, E.I.; Dumesic, J.A. Integrated conversion of hemicellulose and cellulose from lignocellulosic biomass. *Energy Environ. Sci.* **2012**, *6*, 76–80. [[CrossRef](#)]
55. Binder, J.B.; Blank, J.J.; Cefali, A.V.; Raines, R.T. Synthesis of Furfural from Xylose and Xylan. *ChemSusChem* **2010**, *3*, 1268–1272. [[CrossRef](#)]

Disclaimer/Publisher’s Note: The statements, opinions and data contained in all publications are solely those of the individual author(s) and contributor(s) and not of MDPI and/or the editor(s). MDPI and/or the editor(s) disclaim responsibility for any injury to people or property resulting from any ideas, methods, instructions or products referred to in the content.